CORRELATIONS IN ULTRA-RELATIVISTIC NUCLEAR COLLISIONS WITH STRINGS* **

Martin Rohrmoser[a,†], Wojciech Broniowski[a,b]

[a]Institute of Physics, Jan Kochanowski University, 25-406 Kielce, Poland
[b]H. Niewodniczański Institute of Nuclear Physics
Polish Academy of Sciences, 31-342 Kraków, Poland

(Received July 4, 2019)

While string models describe initial-state radiation in ultra-relativistic nuclear collisions well, they mainly differ in their end-point positions of the strings in spatial rapidity. We present a generic model where wounded constituents are amended with strings whose both end-point positions fluctuate and analyze semi-analytically various scenarios of string-end-point fluctuations. In particular, we constrain the different cases to experimental data on rapidity spectra from collisions at $\sqrt{s_{NN}} = 200$ GeV, and explore their respective two-body correlations, which allows to partially discriminate the possible solutions.

DOI:10.5506/APhysPolBSupp.13.151

Our main goal is to better understand the origin of forward–backward multiplicity fluctuations within ultra-relativistic nuclear collisions. This text is mainly based on our work [1], which generalizes the analysis of [2]. Our approach uses strings with fluctuating end-points together with fluctuations in the number of sources of these strings in order to describe the multiplicity fluctuations.

QCD-motivated string models have been successful in describing soft particle production — in particular Monte Carlo implementations of the Lund model [3–8] or the Dual Parton model involving Pomeron and Regge exchange [9–11]. These models have in common that they assume the formation of numerous strings at early stages of nuclear collisions. These strings represent the confined color fields spanned between two opposite

* Presented at "Excited QCD 2019", Schladming, Austria, January 30–February 3, 2019.

** Supported by the National Science Centre, Poland (NCN) grant 2015/19/B/ST/00937.

† Corresponding author: Martin.Rohrmoser@ujk.edu.pl

color charges. Breakings of these strings correspond to particle–antiparticle creation and accounts for the large multiplicity creation at the early stages of nuclear collisions. However, distributions of string-end points vary between the different approaches. Thus, we also try to understand the phenomenological consequences of different string-end-point distributions.

On the other hand, the produced multiplicity can be successfully described within the wounded picture [12]. In particular, the wounded constituent model [13–16] works remarkably well in the description of RHIC data. The wounded picture describes the $\frac{\mathrm{d}N}{\mathrm{d}\eta}$ spectra via the creation of a number of sources within the Glauber model [17] which all emit particles following a common emission profile $f(\eta)$.

Before merging the two models, we will outline the wounded constituent model, which we write as

$$\frac{\mathrm{d}N}{\mathrm{d}\eta} = \langle N_A \rangle f(\eta) + \langle N_B \rangle f(-\eta)\,, \tag{1}$$

where N_A and N_B are the number of wounded constituents. For our numerical results, these numbers were obtained by GLISSANDO [18], a Monte Carlo simulation code of the Glauber model, where it was assumed that every nucleon can provide up to three wounded constituents.

We verified the scaling behavior of Eq. (1) by extracting from experimental data an emission profile, which does not depend on the number of sources. Figure 1 shows an example for experimental data from PHOBOS [19, 20] on d–Au collisions. As it can be seen, the extracted emission profiles overlap within the uncertainties propagated from experiment, so that a description of rapidity spectra with a universal emission profile $f(\eta)$ can be justified. We thus confirm the results by [21].

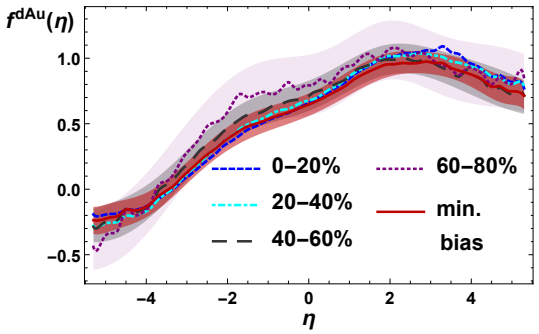

Fig. 1. (Color online) Emission profiles from PHOBOS data [19, 20] on d–Au collisions at $\sqrt{s_{NN}} = 200$ GeV. Experimental uncertainties have been propagated for the 40–60% and 60–80% centrality classes and the minimum bias case (colored bands).

We also verified whether it is possible to reproduce both spectra for d–Au and Au–Au collisions, comparing to PHOBOS data [19, 20, 22]. To this end, we used an emission profile $f(\eta)$ with a symmetric part obtained from Au–Au and an asymmetric part obtained from d–Au collisions, and could reproduce the qualitative behavior of the spectra. We will use this particular version of $f(\eta)$ in the remainder of the text.

The wounded constituent model is combined with a generic string model, where each wounded source pulls exactly one string in pseudo-rapidity with end-points y_1 and y_2. The strings are assumed to break at least once, which yields particle emission at pseudo-rapidity η, which follows for each string individually a radiation profile $s(\eta; y_1, y_2)$. For simplicity, we assume uniform probability for particle emission, *i.e.*,

$$s(\eta; y_1, y_2) = \omega \left[\theta(y_1 < \eta < y_2) + \theta(y_2 < \eta < y_1)\right] , \tag{2}$$

where ω is the production rate.

We use string-end-point distributions $g_1(y_1)$ and $g_2(y_2)$ for which we demand that they allow to reproduce the one-body-emission profile $f(\eta)$ extracted from experiment. Thus, we find that

$$f(\eta) = \int_{-\infty}^{\infty} \mathrm{d}y_1\, g_1(y_1) \int_{-\infty}^{\infty} \mathrm{d}y_2\, g_2(y_2) s(\eta, y_1, y_2) = \omega \left[\tfrac{1}{2} - 2H_1(\eta)H_2(\eta)\right] , \tag{3}$$

with the shifted cumulative distribution function defined as

$$H_i(\eta) = G_i(\eta) - \tfrac{1}{2} , \qquad G_i(\eta) = \int_{-\infty}^{\eta} \mathrm{d}y\, g_i(y) , \qquad i = 1, 2 , \tag{4}$$

It is clear from Eq. (3) that choices for $H_1(\eta)$ and $H_2(\eta)$ are not unique. However, since $H_1(\eta), H_2(\eta) \in [-\frac{1}{2}, \frac{1}{2}]$, one can infer $\omega \in [f(\eta_{\max}), 2f(\eta_{\max})]$, where $\eta_{\max}$ is the position in pseudo-rapidity of the maximum of $f(\eta)$. We study the following three cases of solutions to Eq. (3):

1. $\omega = 2f(\eta_{\max})$ (we label the case "$g_1 = g_2$"), where one obtains

$$H_1(\eta) = H_2(\eta) = \sqrt{\frac{1}{4} - \frac{1}{2\omega} f(\eta)}\, \mathrm{sgn}(\eta - \eta_{\max}) . \tag{5}$$

2. $\omega = f(\eta_{\max})$ (labeled "disjoint case"), where one obtains

$$\begin{aligned} H_1(\eta) &= -\frac{1}{2}\theta(\eta_{\max} - \eta) + \left[\frac{1}{2} - \frac{1}{\omega} f(\eta)\right] \theta(\eta - \eta_{\max}) , \\ H_2(\eta) &= -\left[\frac{1}{2} - \frac{1}{\omega} f(\eta)\right] \theta(\eta_{\max} - \eta) + \frac{1}{2}\theta(\eta - \eta_{\max}) . \end{aligned} \tag{6}$$

3. An intermediate case, where $f(\eta_{\max}) < \omega < 2f(\eta_{\max})$. There, $H_1(\eta)$ is assumed as fixed and one obtains

$$H_2(\eta) = \frac{\frac{1}{4} - \frac{1}{2\omega} f(\eta)}{H_1(\eta)} \,. \tag{7}$$

One can conclude from Eq. (3) that the solutions for $H_1(\eta)$ and $H_2(\eta)$ in the disjoint case serve as upper and lower limits for all other solutions to Eq. (6). Figure 2 shows results for $g_1(\eta)$ and $g_2(\eta)$ as well as $G_1(\eta)$ and $G_2(\eta)$.

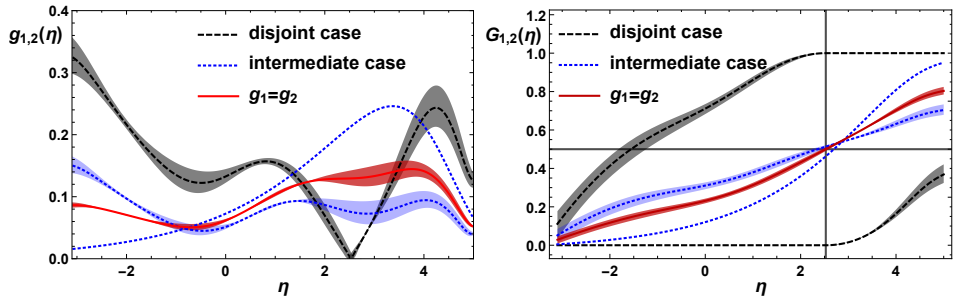

Fig. 2. The three solutions for string-end-point distribution functions (left) discussed in the text together with their cumulative distribution functions (right).

Equation (3) can be generalized to obtain the density $f_2(\eta_1, \eta_2)$ for the emission of particle pairs at pseudo-rapidities η_1 and η_2 as [1]

$$f_2(\eta_1, \eta_2) = \omega^2 G_1[\min(\eta_1, \eta_2)] \{1 - G_2[\max(\eta_1, \eta_2)]\} + (1 \leftrightarrow 2) \,. \tag{8}$$

Summing over all possible sources, one can obtain the covariance for the emission of particle pairs in nuclear collisions as

$$\begin{aligned} \mathrm{cov}_{AB}(\eta_1, \eta_2) \;=\; & \langle N_A \rangle \,\mathrm{cov}(\eta_1, \eta_2) + \langle N_B \rangle \,\mathrm{cov}(-\eta_1, -\eta_2) \\ & + \mathrm{var}(N_A) f(\eta_1) f(\eta_2) + \mathrm{var}(N_B) f(-\eta_1) f(-\eta_2) \\ & + \mathrm{cov}(N_A, N_B) \left[f(\eta_1) f(-\eta_2) + f(-\eta_1) f(\eta_2) \right] , \end{aligned} \tag{9}$$

with $\mathrm{cov}(\eta_1, \eta_2) = f_2(\eta_1, \eta_2) - f(\eta_1) f(\eta_2)$. One can also define the correlations C as

$$C_{AB}(\eta_1, \eta_2) = 1 + \frac{\mathrm{cov}_{AB}(\eta_1, \eta_2)}{f_{AB}(\eta_1) f_{AB}(\eta_2)} \,, \qquad \text{with} \quad f_{AB}(\eta) := \frac{\mathrm{d}N}{\mathrm{d}\eta} \,. \tag{10}$$

One can define a_{nm} coefficients [23] as projections of $C_{AB}(\eta_1, \eta_2)$ on $T_n(x) = \sqrt{n + 1/2} P_n(x)$ (with Legendre polynomials $P_n(x)$)

$$a_{nm} = \frac{\int_{-Y}^{Y} \mathrm{d}\eta_1 \int_{-Y}^{Y} \mathrm{d}\eta_2 \, C_{AB}(\eta_1, \eta_2) \, T_n\left(\frac{\eta_1}{Y}\right) T_m\left(\frac{\eta_2}{Y}\right)}{\int_{-Y}^{Y} \mathrm{d}\eta_1 \int_{-Y}^{Y} \mathrm{d}\eta_2 \, C_{AB}(\eta_1, \eta_2)} \,, \tag{11}$$

with the covered pseudo-rapidity range $[-Y, Y]$, where we use $Y = 1$ for RHIC. Results for a_{11} are shown in Fig. 3. They scale to a good approximation as the inverse number of sources, as can be expected from Eqs. (9)–(11). Furthermore, the $g_1 = g_2$ case differs from the disjoint case by almost a factor of 3, while it is practically indistinguishable from the intermediate case.

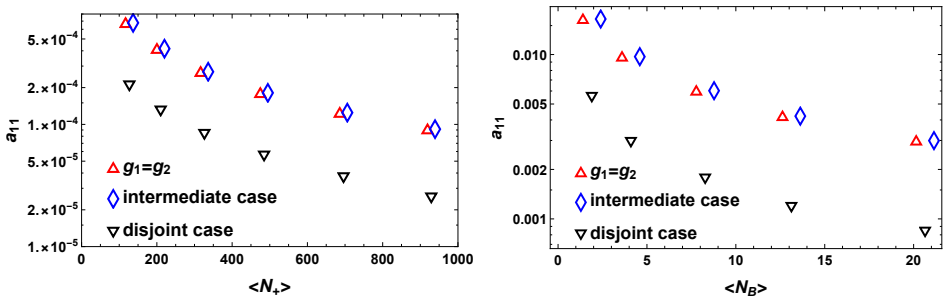

Fig. 3. Legendre coefficients a_{11} for Au–Au (left) and d–Au collisions (right) at $\sqrt{s_{NN}} = 200$ GeV as a function of the number of sources, where $N_+ = N_A + N_B$.

We summarize our main findings:

1. Our semianalytic approach merges a wounded constituent model with a string model. We constrained the model to reproduce the one-body spectra in pseudo-rapidity.

2. A family of possible solutions to the string-end-point distributions exists. However, they can be further discriminated (at least for the two limiting cases) via two-particle correlations in rapidity.

3. The Legendre coefficients a_{nm} of the correlations approximately scale as the inverse of the number of sources, as expected.

REFERENCES

[1] M. Rohrmoser, W. Broniowski, *Phys. Rev. C* **99**, 024904 (2019) [arXiv:1809.08666 [nucl-th]].

[2] W. Broniowski, P. Bożek, *Phys. Rev. C* **93**, 064910 (2016) [arXiv:1512.01945 [nucl-th]].

[3] B. Andersson, G. Gustafson, G. Ingelman, T. Sjöstrand, *Phys. Rep.* **97**, 31 (1983).

[4] X.-N. Wang, M. Gyulassy, *Phys. Rev. D* **44**, 3501 (1991).

[5] Z.-W. Lin *et al.*, *Phys. Rev. C* **72**, 064901 (2005) [arXiv:nucl-th/0411110].

[6] T. Sjöstrand *et al.*, *Comput. Phys. Commun.* **191**, 159 (2015) [arXiv:1410.3012 [hep-ph]].

[7] C. Bierlich, G. Gustafson, L. Lönnblad, H. Shah, *J. High Energy Phys.* **1810**, 134 (2018) [arXiv:1806.10820 [hep-ph]].

[8] S. Ferreres-Solé, T. Sjöstrand, *Eur. Phys. J. C* **78**, 983 (2018) [arXiv:1808.04619 [hep-ph]].

[9] A. Capella, U. Sukhatme, C.-I. Tan, J. Tran Thanh Van, *Phys. Rep.* **236**, 225 (1994).

[10] K. Werner *et al.*, *Phys. Rev. C* **82**, 044904 (2010) [arXiv:1004.0805 [nucl-th]].

[11] T. Pierog *et al.*, *Phys. Rev. C* **92**, 034906 (2015) [arXiv:1306.0121 [hep-ph]].

[12] A. Białas, M. Błeszyński, W. Czyż, *Nucl. Phys. B* **111**, 461 (1976).

[13] A. Białas, W. Czyż, W. Furmański, *Acta Phys. Pol. B* **8**, 585 (1977).

[14] A. Białas, K. Fiałkowski, W. Słomiński, M. Zieliński, *Acta Phys. Pol. B* **8**, 855 (1977).

[15] A. Białas, W. Czyż, *Acta Phys. Pol. B* **10**, 831 (1979).

[16] V.V. Anisovich, Yu.M. Shabelski, V.M. Shekhter, *Nucl. Phys. B* **133**, 477 (1978).

[17] R.J. Glauber, in: *Lectures in Theoretical Physics*, Vol. 1, W.E. Brittin, L.G. Dunham (Eds.), Interscience, New York 1959, p. 315.

[18] M. Rybczyński, G. Stefanek, W. Broniowski, P. Bożek, *Comput. Phys. Commun.* **185**, 1759 (2014) [arXiv:1310.5475 [nucl-th]].

[19] B.B. Back *et al.* [PHOBOS Collaboration], *Phys. Rev. Lett.* **93**, 082301 (2004) [arXiv:nucl-ex/0311009].

[20] B.B. Back *et al.* [PHOBOS Collaboration], *Phys. Rev. C* **72**, 031901(R) (2005) [arXiv:nucl-ex/0409021].

[21] M. Barej, A. Bzdak, P. Gutowski, *Phys. Rev. C* **97**, 034901 (2018) [arXiv:1712.02618 [hep-ph]].

[22] B.B. Back *et al.*, *Phys. Rev. Lett.* **91**, 052303 (2003) [arXiv:nucl-ex/0210015].

[23] A. Bzdak, D. Teaney, *Phys. Rev. C* **87**, 024906 (2013) [arXiv:1210.1965 [nucl-th]].